

# Atmospheric Pattern Correlates of Human Brain Structure

Max Korbmacher <sup>1,2,3\*</sup>, Ole A. Andreassen <sup>4,5</sup>, Lars T. Westlye <sup>4,6</sup>, Ivan I. Maximov <sup>2</sup>, Ivan Kuznetsov <sup>7</sup>

<sup>1</sup>Neuro-SysMed, Department of Neurology, Haukeland University Hospital, Norway.

<sup>2</sup>Department of Health and Functioning, Western Norway University of Applied Sciences, Norway.

<sup>3</sup>Mohn Medical Imaging and Visualisation centre, Department of Radiology, Haukeland University Hospital, Norway.

<sup>4</sup>Center for Precision Psychiatry, University of Oslo and Oslo University Hospital, Norway.

<sup>5</sup>K.G. Jebsen Centre for Neurodevelopmental disorders, University of Oslo, Norway.

<sup>6</sup>Department of Psychology University of Oslo, Norway.

<sup>7</sup>Alfred Wegener Institute, Helmholtz Centre for Polar and Marine Research, Bremerhaven, Germany.

\*Correspondence Author: Claudio Jimenez, Departamento de Neurología, Hospital Simón Bolívar, Subred Integrada de Servicios de Salud del Norte E.S.E.

Received Date: May 05, 2025| Accepted Date: May 25, 2025| Published Date: June 19, 2025

**Citation:** Max Korbmacher, Ole A. Andreassen, Lars T. Westlye, Ivan I. Maximov, Ivan Kuznetsov, et al, (2025), Atmospheric Pattern Correlates of Human Brain Structure, *Clinical Research and Reviews*,4(3); DOI:10.31579/2835-8376/044.

**Copyright:** © 2025, Max Korbmacher. this is an open-access article distributed under the terms of the Creative Commons Attribution License, which permits unrestricted use, distribution, and reproduction in any medium, provided the original author and source are credited.

## Abstract

Climate change increasingly impacts human health, yet its neurobiological effects remain poorly understood. Analysing structural neuroimaging data of 30,831 UK participants (4,294 with follow-up assessments), we show that ambient weather conditions (warm, sunny, low precipitation and wind speed) associate with brain structure variations that exceed contributions from Alzheimer's disease genetic risk scores and self-reported mental health. These findings establish atmospheric patterns as measurable environmental correlates of brain structure and reveal new pathways for understanding climate-brain interactions.

**Keywords:** traumatic brain injury; vitamin D; vitamin E; neuroprotection; systematic review; meta- analysis

## Introduction

Despite growing concerns about climate change impacts on human health and well-being, 1,2 evidence linking atmospheric conditions to brain structure remains limited. This knowledge gap persists partly due to the challenges of integrating large-scale meteorological data with neuroimaging cohorts. Atmospheric variability (temperature, precipitation, solar radiation, wind) may influence brain structure through multiple pathways, including effects on multiple bodily systems, 2 physical activity, 3 vitamin D synthesis,4 circadian rhythms.5 Given projections of increased climatic

variability and extreme weather events,6 understanding neurobiological sensitivity to atmospheric exposures could inform preventive strategies and help anticipate neurological health burdens associated with climate change.1 Hence, an improved understanding of associations between atmospheric patterns and brain structure is essential as environmental conditions continue to shift both globally and locally. Here, we provide a first step towards investigating atmospheric-brain associations, establishing brain structural correlates of meteorological conditions in the United Kingdom.

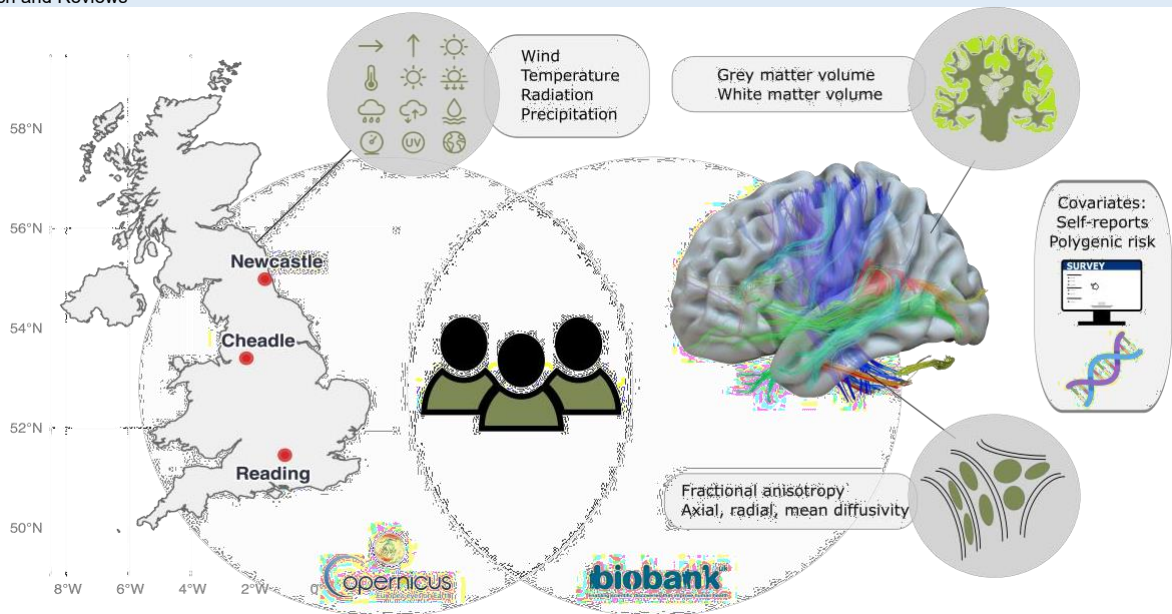


**Figure:1: Study design: Monthly meteorological data were linked to structural brain imaging (N = 30,831), yielding measures of grey matter volume, white matter volume, and white matter microstructure (diffusion metrics). Genetic risk scores and self-reported mental health data served as comparison variables.**

We linked atmospheric data averaged over the United Kingdom for the month preceding the health and MRI assessments (Fig. 1). The derived averaged atmospheric indices were joined with individuals' brain metrics for all 30,831 participants at baseline (see Table 1 in the Online Methods for an overview of key variables), and for n=4,294 at follow-up (Supplemental Table 1). As a comparison to atmospheric variables as predictors of brain structure, we also used self-reports of mental health, correspondingly polygenic risk scores (PGRS) of Alzheimer's Disease, considering the sample age. our analyses, all corrected for assessment site, household income, sex, age, intracranial volume, and surface holes, revealed that

atmospheric variables presented stronger associations (median±mean absolute deviation (MAD)  $|\beta| = 0.013 \pm 0.013$ ) with brain structure than PGRS of Alzheimer's disease (AD, median±MAD  $|\beta| = 0.006 \pm 0.001$ ), and on average similar to self-reports of neuroticism and depression ( $|\beta| = 0.013 \pm 0.012$ ; see Fig. 2; Supplemental Data 1). However, the strongest associations were found for atmospheric variables for associations between fractional anisotropy and a) 10 metre wind speed (standardized effect size  $\beta = -0.059$ , 95% CI [-0.068, -0.049], pFDR=1.78\*10<sup>-30</sup>), and surface downward UV radiation ( $\beta = 0.055$ , 95% CI [0.045, 0.064], pFDR=4.42\*10<sup>-27</sup>).

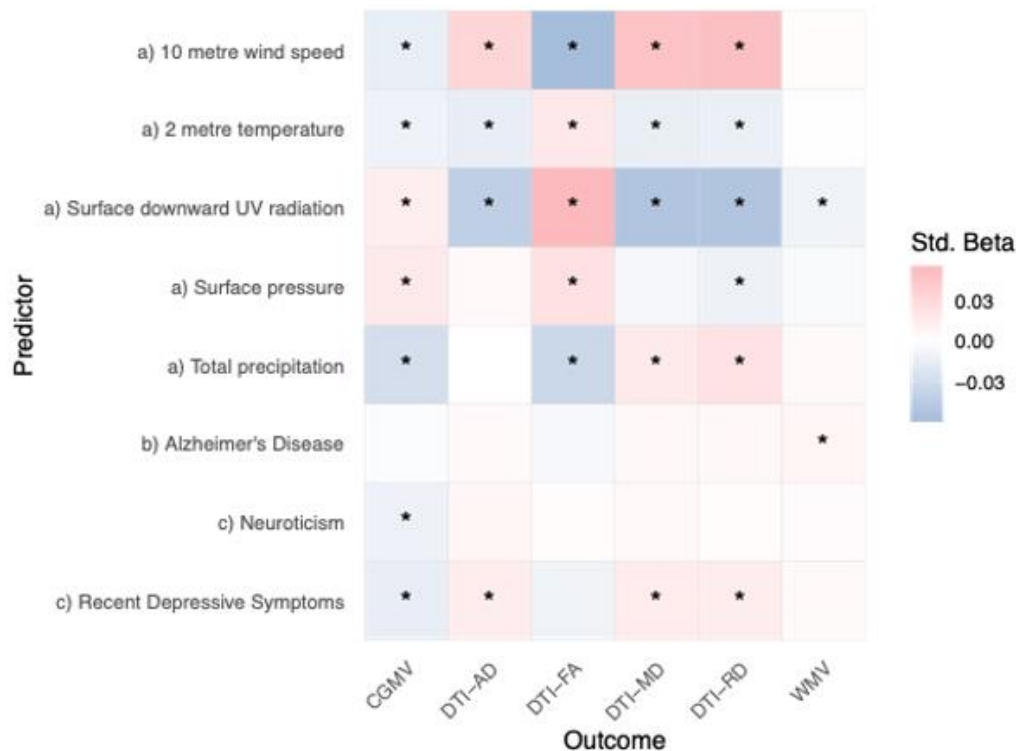


**Figure 2: Associations between brain structural and a) atmospheric indicators, b) polygenic risk of Alzheimer's disease, and c) self-reports of recent depression and neuroticism.**

PGRS = polygenic risk score, CGMV = cortical grey matter volume, DTI = diffusion tensor imaging, AD = axial diffusivity, FA = fractional anisotropy, MD = mean diffusivity, RD = radial diffusivity, WMV = white matter volume. Std. Beta = standardized beta or regression coefficients. The associations suggest that better weather (lower precipitation, lower wind speed, higher short- and long-wave radiation and higher surface pressure) was associated with greater cortical volume and higher fractional anisotropy (indicating anisotropy of water diffusion along a single direction and thereby structural integrity of axonal bundles), in addition to lower axial, radial and mean diffusivity (indicating the magnitude of diffusivity, along or perpendicular to the fibre bundles or their average) (Figure. 2). Likelihood Ratio Tests suggested that adding AD PGRS or self-reported outcomes on recent depression and neuroticism did not improve models predicting brain structure. Changes to the model were non-significant when adding the covariates ( $p > 0.05$ ) in 65 of 90 (27.78%) of the models with FDR-adjustment for multiple comparisons. Adding neuroticism to the models explaining cortical volume presented the largest contribution ( $26.12 < F < 27.16$ ,  $p < 0.05$ ), followed by neuroticism ( $11.29 < F < 11.89$ ,  $p < 0.05$ ; see Supplemental Data 2). However, while statistically significant the added variance of AD PGRS and self-reported outcomes was low ( $\Delta R^2 < 0.03\%$ ). Note that the pattern of associations was also found over time, using mixed linear models considering both timepoints, in the  $n = 4,294$  participants with follow-up scans (Supplemental Figure 1, Supplemental Data 3). Here, the effects of total precipitation were strongest, associating negatively with cortical volume ( $\beta = -0.051$ , 95% CI  $[-0.053, -0.048]$ ,  $pFDR < 2.23 \times 10^{-308}$ ) and fractional anisotropy ( $\beta = -0.048$   $[-0.051, -0.046]$ ,  $pFDR < 2.23 \times 10^{-308}$ ), and positively associating with mean diffusivity ( $\beta = 0.043$   $[0.039, 0.047]$ ,  $pFDR = 2.81 \times 10^{-108}$ ) and radial diffusivity ( $\beta = 0.043$   $[0.039, 0.046]$ ,  $pFDR = 4.93 \times 10^{-140}$ ).

Finally, considering that the strongest cross-sectional and longitudinal associations between atmospheric conditions and whole-brain variables were found for precipitation, surface pressure and wind speed (compare Figure 2, Supplemental Figure 1), we assessed associations of these variables with tract- and region-level brain metrics (Supplemental Figures 2-4). For both associations, white matter microstructure was more sensitive to weather phenomena. Yet also the volume of the amygdala and ventricles were among the strongest correlates of total precipitation (Supplemental Figure 2). Across associations between tracts and regional brain characteristics, atmospheric conditions, genetic, and behavioural scores, diffusivity in the inferior longitudinal fasciculus presented the strongest associations ( $\beta < 0.08$ ) with multiple atmospheric variables (for a full overview across associations see Supplemental Data 4). Atmospheric patterns were associated with markers of brain structure, with effect sizes generally exceeding those of AD PGRS, as well as mental health self-reports. Ambient atmospheric patterns, defined by lower precipitation and wind speed and higher temperature, solar radiation and atmospheric pressure, corresponded to higher cortical volume, greater fractional anisotropy, and lower white matter diffusivity at baseline and over time. These findings demonstrate a measurable link between meteorological conditions and brain structure. Several biological mechanisms may underlie the examined weather-brain associations. Solar radiation exposure, positively associated with structural integrity, could act through vitamin synthesis or circadian regulation affecting neuroplasticity and cellular maintenance. Atmospheric pressure and precipitation may influence brain structure indirectly via behavioural pathways, as favourable weather supports outdoor activity, social engagement, and exposure to natural environments,<sup>7,8</sup> all being factors linked to general and brain health.<sup>9,10</sup> High-pressure systems are also associated with low dispersion and hence air pollution,<sup>11</sup> which is in turn associated with neurotoxic burden,<sup>12</sup> resulting in increased AD risk.<sup>13,14</sup> Confounding effects from

third variables and limitations to measurements must also be considered. Despite adjustment for multiple covariates, atmospheric patterns and brain structure covary with unmeasured socioeconomic and lifestyle factors. Differences in urbanicity, healthcare access, diet, occupation, and cultural practices can all influence brain structure as well as direct and indirect exposure to atmospheric conditions. Individuals with greater resources may mitigated adverse weather through housing, transport, or relocation. The observed associations may therefore partly reflect interactions between meteorological and social determinants that were not captured by our models. Moreover, unmeasured confounders (beyond scanner site, household income, sex, age, ICV, and surface holes) may also contribute to both weather exposure and brain outcomes. Weather data averaged across the United Kingdom mask local microclimatic variation and individual exposure differences. Time spent outdoors, indoor conditions, vitamin D supplementation, circadian rhythm, and air pollution exposure were not captured. The one-month averaging window, while pragmatic, may not reflect the most relevant temporal scale for structural effects. The cohort's geographic and demographic composition further limits generalisability. Namely, the UK Biobank imaging sample is composed of middle-aged and older adults in relatively good health, not representative of the general UK population. Non-linearity and boundary effects may also exist, potentially limiting the generalisability of this study. Extreme weather or long-term cumulative exposure may have distinct impacts from the monthly means analysed here. Seasonal cycles could exert neurobiological influences distinct from stochastic weather variation. However, a previous multi-scanning case study suggests that brain structure estimates are relatively robust to seasonal effects.<sup>15</sup> Nevertheless, individual differences in weather sensitivity, shaped by genetic, developmental, or health factors, were not examined but may modulate these relationships. Our findings have implications for neuroscience and public health. Longitudinal designs are needed to establish temporal precedence, assess reversibility, and quantify dose-response relationships. Such studies could clarify whether within-person variation in weather exposure predicts brain structural change and identify sensitive exposure windows. Future research should also examine regional specificity, vulnerable populations, and potential modifiers such as outdoor time, activity levels, social engagement, and baseline health.

Integrating wearable sensor data would improve exposure assessment beyond aggregated meteorological indices. If causal relationships are confirmed, the findings could inform interventions. Urban planning and building design might incorporate strategies to mitigate negative weather effects on neurological health. Individual-level interventions, including light therapy, vitamin D supplementation, or structured activity during unfavourable weather, warrant investigation. As global climate change alters weather variability and extremes, understanding the neurobiological systems sensitive to meteorological variation becomes critical for anticipating and mitigating future health burdens. In summary, recent ambient weather patterns are associated with human brain structure, with effect sizes exceeding those of frequently applied PGRS for common mental and brain disorders and self-reported mental health measures. These data provide an empirical foundation for environmental neuroscience linking climate variability to brain biology. While causal mechanisms remain to be established, the results suggest that meteorological conditions are neurobiologically relevant and should be integrated into models of brain health as global environmental conditions continue to shift.

## Online Methods

### Sample

We extracted multimodal (T1-weighted and diffusion-weighted images) MRI data from the UK Biobank database.<sup>16</sup> We excluded participants diagnosed with any mental and behavioural disorder (ICD-10 category F), disease of the nervous system (ICD-10 category G), and disease of the

circulatory system (ICD-10 category I), or stroke. Weather data, PGRS and self-reported data were merged, resulting in N = 30,831 included participants (sample overview at baseline: Table 1; at follow-up: Supplemental Table 1).

Characteristic	Cheadle, N = 18,018 <sup>1</sup>	Newcastle, N = 8,260 <sup>1</sup>	Reading, N = 4,553 <sup>1</sup>
<i>Demographics</i>			
Age (years)	65 (58, 70)	66 (60, 72)	68 (61, 73)
Male (sex)	8,752 (49%)	3,888 (47%)	2,204 (48%)
<i>Income in £1,000</i>			
Less than 18	1,930 (11%)	905 (11%)	269 (5.9%)
18-31	3,889 (22%)	1,667 (20%)	710 (16%)
31-52	5,089 (28%)	2,308 (28%)	1,072 (24%)
52-100	4,512 (25%)	2,152 (26%)	1,425 (31%)
More than 100	928 (5.2%)	563 (6.8%)	702 (15%)
Don't know	336 (1.9%)	145 (1.8%)	92 (2.0%)
No answer	1,192 (6.7%)	502 (6.1%)	276 (6.1%)
Intracranial Volume (litres)	1.5 (1.4, 1.6)	1.5 (1.4, 1.6)	1.5 (1.4, 1.6)
Surface Holes	53 (38, 75)	50 (36, 74)	44 (33, 62)
Fractional Anisotropy	0.46 (0.45, 0.47)	0.46 (0.44, 0.47)	0.46 (0.45, 0.47)
Mean Diffusivity	0.89 (0.87, 0.91)	0.89 (0.87, 0.91)	0.89 (0.87, 0.91)
Radial Diffusivity	0.65 (0.62, 0.67)	0.65 (0.62, 0.67)	0.64 (0.62, 0.67)
Axial Diffusivity	1.38 (1.36, 1.40)	1.37 (1.35, 1.39)	1.38 (1.36, 1.40)
Cortical Volume (litres)	0.4 (0.4, 0.5)	0.4 (0.4, 0.5)	0.4 (0.4, 0.5)

**Table 1: Sample characteristics at baseline.**

### MRI Acquisition and Processing

The MRI acquisition protocol has been described previously (<https://www.fmrib.ox.ac.uk/ukbiobank/protocol/>).<sup>16</sup> Starting with the diffusion MRI data, we processed these imaging data using an optimised pipeline,<sup>17</sup> which entails corrections of noise, Gibbs ringing, susceptibility-induced and motion distortions, and eddy current induced artifacts. Isotropic 1 mm<sup>3</sup> Gaussian smoothing was applied using fslmaths (FSL version 6.0.1).<sup>18</sup> We estimated diffusion tensors at each voxel, or Diffusion Tensor Imaging (DTI),<sup>19</sup> but used a signal decomposition in order to take into account kurtosis imaging as well. This procedure has been shown to lead to more robust and reproducible DTI estimates.<sup>20</sup> We employed Tract-based Spatial Statistics<sup>21</sup> for the analysis of white matter integrity. The first step was to align the fractional anisotropy (FA) images to standard MNI space using non-linear registration. A mean FA image and corresponding skeleton were then generated from the aligned data. Each diffusion parameter map was subsequently projected onto this mean FA skeleton. We then averaged the respective DTI metrics FA, axial, radial and mean diffusivity across the white matter skeleton. We used the YTTTRIUM method<sup>22</sup> for quality control of diffusion MRI scalars. For YTTTRIUM global diffusion MRI scalar metrics are converted into 2-dimensional format using a structural similarity extension of each scalar map to their mean image to create a 2D distribution of image and diffusion parameters. Non-clustering values are then excluded. For T1-weighted MRI data, we used Free Surfer version 5.3.0 for surface-based reconstruction and estimation of brain grey and white matter and intracranial volumes, in addition surface holes, which have previously been shown to be crucial to avoid bias in large sample brain image analyses.<sup>23</sup> We used Euler numbers<sup>24</sup> to exclude images when the Euler number exceeded three standard deviations from the mean. Finally, to allow for more spatially specific assessment of brain structure, we parcellated both grey and white matter. For the T1-weighted MRI-derived volumes, we used the Desikan-Killiany Atlas<sup>25</sup> to obtain regional estimates of brain volumes, leading to a total of 68 brain features based on the 34 regions of interest for each brain hemisphere. We used the 20 tracts from the John Hopkins University atlas<sup>26</sup> which are based on a probabilistic WM atlas. We

averaged across the 20 tracts for each of the 4 DTI parameters, totalling 80 values per individual.

### Polygenic risk

We estimated the polygenic risk score (PGRS) for each participant with available genomic data, using LDpred227 with default settings. As input for the PGRS, we used the summary statistics from a recent genome-wide association study (GWAS) of Alzheimer's Disease (AD),<sup>28</sup> using a minor allele frequency of 0.05. We selected AD PGRS as it is based on a well-powered GWAS<sup>28</sup> and has, as the most common neurodegenerative disease, real-world applicability, particularly considering the examined ageing sample. A previous study also presented relatively strong associations between a PGRS of late onset AD and brain structure.<sup>29</sup>

### Self-reported measures of mental health

We assessed two self-reported measures reflecting state- and trait-level characteristics of mental health: recently experienced depression and the personality trait neuroticism.<sup>30</sup> To assess depression, we used the Recent Depressive Symptoms (RDS-4) score (range: 4-16), which contains four questions covering four dimensions of depression: mood, disinterest, restlessness, and tiredness. The score is computed as a sum of the 4-point Likert-like responses from the four items. The Eysenck Personality Questionnaire-Revised Short Form, which includes 12 items, was used to assess neuroticism. A sum score was computed from the binary responses to the 12 items, where symptoms were either present or absent. Both scores were previously validated against other corresponding scales using test-retest data of the UK Biobank imaging subsample and recommended to be used to assess imaging biomarkers in the context of mental health.<sup>30</sup>

### Atmospheric data

Monthly meteorological data were obtained from the ERA5 reanalysis dataset,<sup>31</sup> specifically the monthly averaged single-level product prior scanning, accessed via the Copernicus Climate Data Store.<sup>32</sup> These data are based on historical observations with a numerical weather prediction model to produce a spatially and temporally complete reconstruction of the



atmosphere over extended periods (~70+ years). Unlike raw observational records, which are irregularly distributed in space and time, reanalysis provides globally gridded fields on a regular mesh, serving as a proxy for the actual atmospheric state. This dataset captures both long-term climate trends and natural variability, making it suitable for investigations of climate patterns, extremes, and variability. In contrast, ensemble means of general circulation models primarily represent the forced climate signal, with much of the natural variability averaged out. Importantly, we used ERA5 reanalysis as a representation of observed atmospheric conditions, rather than relying on weather forecasts or purely modelled climate projections. For

each parameter, spatial means were computed over the broader United Kingdom area (60°–50°N, 7°W–1°E) to derive regional time series for analysis. The greater grid was selected for more accurate measures of atmospheric variables (in contrast to smaller scale local parameters). As a result, the following climate metrics were used for the analysis: the wind speed 10 metres above the Earth’s surface in m/s (10metre wind speed), the 2-metre temperature in Kelvin, 24-hour surface downward ultraviolet (UV) radiation in J\*m-2, the surface pressure in Pascal, and the total precipitation in kg m-2 s-1.

Characteristic	N = 30,831 <sup>1</sup>
Wind speed (m/s)	6.67 (5.71, 7.53)
Temperature in Kelvin	282.9 (280.5, 286.5)
Surface pressure in Pascal	100,673 (100,342, 100,861)
UV radiation in J*m <sup>-2</sup>	1,123,889 (507,593, 2,059,785)
Total precipitation in kg m <sup>-2</sup> s <sup>-1</sup>	0.0031 (0.0024, 0.0036)

Table 2: Atmospheric characteristics at baseline.

Statistical Analyses

First, we ran simple linear models predicting brain variables (B, cortical thickness, fractional anisotropy, radial, axial, and mean diffusivity) from atmospheric patterns or weather variables (W, see Weather Data section) at baseline, controlling for site, household income, sex, age, intracranial volume (ICV), and surface holes (SH). ICV has previously been shown to influence DTI33 and volumetric scalars<sup>34</sup> and needs therefore to be controlled for.

$$B_j = b_0 + b_1W_i + b_2sex + b_3income + b_4age + b_5site + b_6ICV + b_7SH + u \tag{1}$$

Second, we added either psychological and or AD PGRS (PsyG in the formula) separately to each of the estimated models.

$$B_j = b_0 + b_1W_i + b_2sex + b_3income + b_4age + b_5site + b_6ICV + b_7SH + b_8PsyG + u \tag{2}$$

We then used likelihood ratio tests to examine whether the added psychological and genetic factors improved model performance. As supplemental analyses (results are reported in the Supplement), we first show additional baseline and longitudinal associations of PGRS of common psychiatric disorder using formula 2. Second, we report the outcomes from linear mixed effect models mirroring the 2formula 1 but adding follow-up data and a random effect of participant to examine the longitudinal effects for participants for which two scans were available. Among the brain variables  $B_j$ , we also added brain age. Brain age models were trained on the cross-sectional data not entailing the participants from the longitudinal set using a simple linear regression model. This procedure, including strong model performance, has also been described previously.<sup>35</sup> Third, we used the extracted tracts and brain volume average from the Desikan-Killiany atlas to run the same models as presented in formula 1, with the region-and tract-level metrics as the respective dependent variable. The alpha level set at 0.05 was Benjamini-Hochberg corrected to control for the false discovery rate. For comparability, we reported standardised regression coefficients.

Ethics approval

This study was approved by the Norwegian Ethics Commission REK 567301, PVO 17/21624 (Ole Andreassen). The study has been conducted

using UKB data under Application 27412. UKB has received ethics approval from the National Health Service National Research Ethics Service (ref 11/NW/0382).

Declaration of interests

OAA has received a speaker's honorarium from Lundbeck, Janssen, Otsuka and Lilly, and is a consultant to Coretechs.ai and Precision Health. LTW is a minor shareholder of baba. vision.

Data availability

Analysis code can be found at <https://github.com/MaxKorbmacher/WeatherBrain>. ERA5 monthly averaged data on single levels are available from the Copernicus Climate Data Store (<https://cds.climate.copernicus.eu/datasets/reanalysis-era5-single-levels-monthly-means>) (accessed 07 July 2025). Contains modified Copernicus Climate Change Service information 2025. Neither the European Commission nor ECMWF are responsible for any use that may be made of the Copernicus information or data it contains.

Acknowledgements

We want to thank Dennis van der Meer for estimating the polygenic risk scores for the presented analyses. We also want to thank all UK Biobank study facilitators and participants.

References

1. Chen, S. et al. Long-term impacts of heatwaves on accelerated ageing. *Nat. Clim. Chang.* 15, 1000–1007 (2025).

2. Ebi, K. L. et al. Hot weather and heat extremes: health risks. *The Lancet* 398, 698–708 (2021).

3. Aspvik, N. P. et al. Do weather changes influence physical activity level among older adults? - The Generation 100 study. *PLoS One* 13, e0199463 (2018).

4. Buell, J. S. et al. 25-Hydroxyvitamin D, dementia, and cerebrovascular pathology in elders receiving home services. *Neurology* 74, 18–26 (2010).

5. Dunster, G. P. et al. Daytime light exposure is a strong predictor of seasonal variation in sleep and circadian timing of university students. *Journal of Pineal Research* 74, e12843 (2023).

6. Grant, L. et al. Global emergence of unprecedented lifetime exposure to climate extremes. *Nature* 641, 374–379 (2025).
7. Chan, C. B., Ryan, D. A. & Tudor-Locke, C. Relationship between objective measures of physical activity and weather: a longitudinal study. *Int J Behav Nutr Phys Act* 3, 1–9 (2006).
8. Edwards, N. M. et al. Outdoor Temperature, Precipitation, and Wind Speed Affect Physical Activity Levels in Children: A Longitudinal Cohort Study. *J Phys Act Health* 12, 1074–1081 (2015).
9. Twohig-Bennett, C. & Jones, A. The health benefits of the great outdoors: A systematic review and meta-analysis of greenspace exposure and health outcomes. *Environ Res* 166, 628–637 (2018).
10. Kelly, P. et al. Systematic review and meta-analysis of reduction in all-cause mortality from walking and cycling and shape of dose response relationship. *International Journal of Behavioral Nutrition and Physical Activity* 11, 132 (2014).
11. Zhou, M., Xie, Y., Wang, C., Shen, L. & Mauzerall, D. L. Impacts of current and climate induced changes in atmospheric stagnation on Indian surface PM<sub>2.5</sub> pollution. *Nat Commun* 15, 7448 (2024).
12. Block, M. L. & Calderón-Garcidueñas, L. Air pollution: mechanisms of neuroinflammation and CNS disease. *Trends Neurosci* 32, 506–516 (2009).
13. Power, M. C., Adar, S. D., Yanosky, J. D. & Weuve, J. Exposure to air pollution as a potential contributor to cognitive function, cognitive decline, brain imaging, and dementia: A systematic review of epidemiologic research. *NeuroToxicology* 56, 235–253 (2016).
14. Shi, L. et al. Long-term effects of PM<sub>2.5</sub> on neurological disorders in the American Medicare population: a longitudinal cohort study. *Lancet Planet Health* 4, e557–e565 (2020).
15. Wang, M.-Y. et al. The within-subject stability of cortical thickness, surface area, and brain volumes across one year. 2024.06.01.596956 Preprint at <https://doi.org/10.1101/2024.06.01.596956> (2024).
16. Alfaro-Almagro, F. et al. Image processing and Quality Control for the first 10,000 brain imaging datasets from UK Biobank. *NeuroImage* 166, 400–424 (2018).
17. Maximov, I. I., Alnæs, D. & Westlye, L. T. Towards an optimised processing pipeline for diffusion magnetic resonance imaging data: Effects of artefact corrections on diffusion metrics and their age associations in UK Biobank. *Human Brain Mapping* 40, 4146–4162 (2019).
18. Smith, S. M. et al. Advances in functional and structural MR image analysis and implementation as FSL. *NeuroImage* 23, S208–S219 (2004).
19. Bassar, P. J., Mattiello, J. & LeBihan, D. MR diffusion tensor spectroscopy and imaging. *Biophys J* 66, 259–267 (1994).
20. Henriques, R. N., Jespersen, S. N., Jones, D. K. & Veraart, J. Toward more robust and reproducible diffusion kurtosis imaging. *Magnetic Resonance in Medicine* 86, 1600–1613 (2021).
21. Smith, S. M. et al. Tract-based spatial statistics: voxelwise analysis of multi-subject diffusion data. *NeuroImage* 31, 1487–1505 (2006).
22. Maximov, I. I. et al. Fast quality control method for derived diffusion metrics (YTTRIUM) in big data analysis: UK Biobank 18,608 example. *HBM* 42, 3141–3155 (2021).
23. Elyounssi, S. et al. Addressing artifactual bias in large, automated MRI analyses of brain development. *Nat Neurosci* 28, 1787–1796 (2025).
24. Rosen, A. F. et al. Quantitative assessment of structural image quality. *NeuroImage* 169, 407–418 (2018).
25. Desikan, R. S. et al. An automated labeling system for subdividing the human cerebral cortex on MRI scans into gyral based regions of interest. *NeuroImage* 31, 968–980 (2006).
26. Mori, S., Wakana, S., Nagae-Poetscher, L. & Van Zijl, P. MRI atlas of human white matter. *American Journal of Neuroradiology* 27, 1384 (2006).
27. Privé, F., Arbel, J. & Vilhjálmsdóttir, B. J. LDpred2: better, faster, stronger. *Bioinformatics* 36, 5424–5431 (2021).
28. Wightman, D. P. et al. A genome-wide association study with 1,126,563 individuals identifies new risk loci for Alzheimer's disease. *Nat Gen* 53, 1276–1282 (2021).
29. Tank, R. et al. Association between polygenic risk for Alzheimer's disease, brain structure and cognitive abilities in UK Biobank. *Neuropsychopharmacol.* 47, 564–569 (2022).
30. Dutt, R. K. et al. Mental health in the UK Biobank: A roadmap to self-report measures and neuroimaging correlates. *Human Brain Mapping* 43, 816–832 (2022).
31. ERA5 monthly averaged data on single levels from 1940 to present. <https://cds.climate.copernicus.eu/datasets/reanalysis-era5-single-levels-monthly-means?tab=overview>.
32. Buontempo, C. et al. The Copernicus Climate Change Service: Climate Science in Action. *Bulletin of the American Meteorological Society* 103, E2669–E2687 (2022).
33. Eikenes, L., Visser, E., Vangberg, T. & Håberg, A. K. Both brain size and biological sex contribute to variation in white matter microstructure in middle-aged healthy adults. *Hum Brain Mapp* 44, 691–709 (2022).
34. Sanchis-Segura, C., Ibañez-Gual, M. V., Aguirre, N., Cruz-Gómez, Á. J. & Forn, C. Effects of different intracranial volume correction methods on univariate sex differences in grey matter volume and multivariate sex prediction. *Sci Rep* 10, 12953 (2020).
35. Korbacher, M. et al. Cross-Sectional Brain Age Assessments Are Limited in Predicting Future Brain Change. *Human Brain Mapping* 46, e70203 (2025).

**Ready to submit your research? Choose ClinicSearch and benefit from:**

- fast, convenient online submission
- rigorous peer review by experienced research in your field
- rapid publication on acceptance
- authors retain copyrights
- unique DOI for all articles
- immediate, unrestricted online access

**At ClinicSearch, research is always in progress.**

Learn more <https://clinicsearchonline.org/journals/clinical-research-and-reviews>



© The Author(s) 2025. **Open Access** This article is licensed under a Creative Commons Attribution 4.0 International License, which permits use, sharing, adaptation, distribution and reproduction in any medium or format, as long as you give appropriate credit to the original author(s) and the source, provide a link to the Creative Commons licence, and indicate if changes were made. The images or other third party material in this article are included in the article's Creative Commons licence, unless indicated otherwise in a credit line to the material. If material is not included in the article's Creative Commons licence and your intended use is not permitted by statutory regulation or exceeds the permitted use, you will need to obtain permission directly from the copyright holder. To view a copy of this licence, visit <http://creativecommons.org/licenses/by/4.0/>. The Creative Commons Public Domain Dedication waiver (<http://creativecommons.org/publicdomain/zero/1.0/>) applies to the data made available in this article, unless otherwise stated in a credit line to the data.